ACS OMEGA

http://pubs.acs.org/journal/acsodf

Article

Current Regulation and Property Study of Porous Anodic Alumina Films with a Periodic Pore Structure

Tian Lan, Xinjian Xie, Qin Xu,* Qi Peng, Lu Zhang, and Meiyu Dong

Cite This: *ACS Omega* 2021, 6, 7988−7993

Read Online

ACCESS | Metrics & More | Article Recommendations

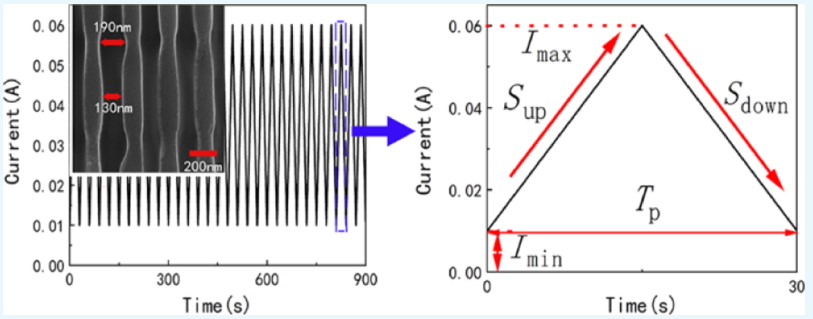

ABSTRACT: Porous anodic alumina (PAA) films with periodically modulated pore diameters are prepared by cyclic anodization of Al in a 0.6 M H_3PO_4 solution at room temperature. Studies have demonstrated that the oscillating current signals have an important effect on the structures of PAA films. Scanning electron microscopy (SEM) images of the PAA film show that when the positive triangle wave current signal is applied, with the increase in the maximum current value, PAA gradually exhibits a symmetrically modulated pore diameter structure, and part of the pores generates slub-like branches. When the maximum current value is 60 mA, the effect of modulation on the pore diameter is the most obvious and the UV reflectance spectrum shows the lowest reflectivity. A sawtooth wave current signal will cause the generation of a V-shaped structure at the junction of adjacent oxide layers. This work provides important guidance for regulating the structure of PAA by changing the current signal.

1. INTRODUCTION

The porous anodic alumina (PAA) film is a kind of nanostructured material with a controllable structure, low cost, and simple preparation process.[1−4] Because of its high-temperature resistance, high stability, optical transmittance, and so on, it has attracted widespread attention in the fields of filtration, catalysis, sensing, storage, separation, template synthesis, energy storage, cell culture, and other fields.[5−8] The traditional PAA film has a precise hexagonal close-packed honeycomb structure and there is a cylindrical air column in the center of each cell.[9] The pores are evenly distributed without crossing and perpendicular to the aluminum base. In recent years, researchers have successfully fabricated some kinds of nanomaterials using traditional PAA templates, such as nanowires, nanotubes, and nanodots.[10−17] With the development of nanoscience, the PAA templates with a single structure cannot meet the needs of production. It has become an important research direction in the field of nanoscience to prepare PAA templates with a special structure by an effective process, which is favored by researchers.[18] Because of the controllability and flexibility of preparation conditions, the PAA templates with special structures can be prepared by changing the conditions of anodization.[19] Traditionally, there are two ways to prepare PAA films: mild anodization (MA) and hard anodization (HA). However, a single way cannot continuously control the pore structure. Therefore, researchers combined MA and HA under different anodization conditions to prepare PAA films with different pore structures. Losic and Losic successfully prepared PAA with unique nanopores with nanohole structures using oscillating current signals.[20] Lee et al. prepared PAA with different pore diameters using pulse anodization.[21] The novel PAA films with a modulated pore diameter not only provide new possibilities for the research of advanced functional materials based on templates but also can be used as models for the study of nanofiltration membranes and sensors.

In this article, we employed the method of cyclic anodization,[22] by applying continuous oscillating current signals in the anodization process, which have different

Received: September 10, 2020
Accepted: November 3, 2020
Published: March 17, 2021

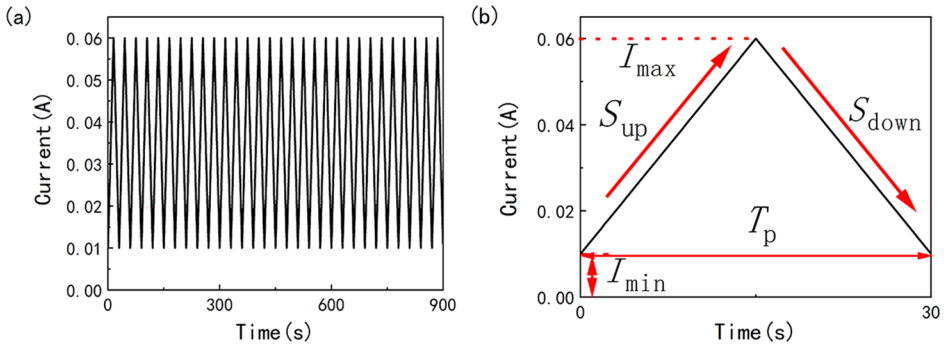

Figure 1. (a) Current (I)−time (t) transient of the positive triangle wave signal showing I_{min} = 10 mA and I_{max} = 60 mA. (b) Graphical definition of the parameters of the positive triangle wave current signal.

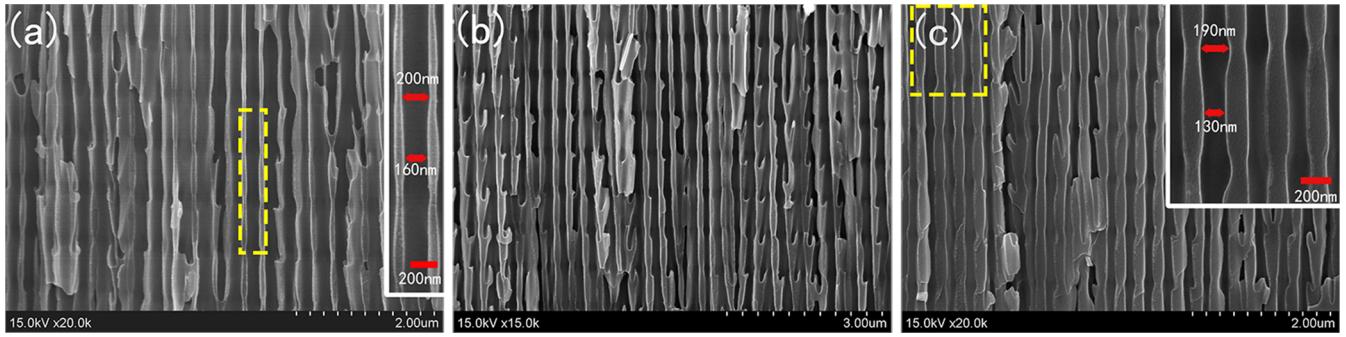

Figure 2. SEM images of the sample prepared using the positive triangle wave current signal (I_{min} = 10 mA and I_{max} = 60 mA). (a) SEM image at the early stage of anodization. (b) SEM image at the middle stage of anodization. (c) SEM image at the latter stage of anodization. [Note: The insets of (a,c) are enlarged images of the yellow dotted frame].

waveforms and amplitudes. Successfully prepared PAA films with a modulated pore diameter structure and V-shaped structure prove that it is feasible to regulate the structure of PAA by changing the current signal.

2. EXPERIMENTAL SECTION

2.1. Aluminum Pretreatment. High-purity (99.99%) aluminum sheets were annealed in a high-temperature (400 °C) environment with argon gas to eliminate stress and then electropolished in a mixture of $HClO_4$ and absolute ethanol for 5 min to remove oil stains and slight scratches. Finally, the aluminum sheets were soaked in a mixed solution of acetone and absolute ethanol for ultrasonic vibration and then dried to remove the polishing liquid on the surface.

2.2. Anodization of Aluminum. At room temperature, PAA films were prepared with different waveform signals in 0.6 M H_3PO_4. The main waveforms are positive triangle waves, discontinuous sawtooth waves, and modified sawtooth waves (the combination of sawtooth waves and sinusoidal waves). The waveforms were made using LabVIEW software, and the power supply is based on a Keithley 2450 digital sourcemeter. We set the minimum current value (i.e., I_{min}) during the experiment to 10 mA. First, a series of samples were prepared using the positive triangle wave current signal, the values of the maximum current (i.e., I_{max}) were 20, 30, 40, 60, 80, and 100 mA, and the anodization period (i.e., T_P) is 30 s for 30 cycles. Then, the sample was prepared using the discontinuous sawtooth wave current signal, I_{max} = 100 mA, T_P = 60 s, and 30 cycles. The last sample was prepared using the modified sawtooth wave current signal, I_{max} = 100 mA, T_P = 100 s, and 10 cycles.

2.3. Characterization. All samples were etched in a saturated $CuCl_2$ solution to remove the aluminum substrate. LabVIEW software was utilized to record the I−t and U−t curves during the experiment. A Hitachi S-4800 scanning electron microscope was employed for the microstructure characterization of the samples. UV−vis reflectance spectra of the films were recorded on a UV-3600 spectrophotometer.

3. RESULTS AND DISCUSSION

The anodization mode was set to the positive triangle wave current pulse signal. In this process, the current was moved between high and low current values (i.e., I_{max} and I_{min}) following a positive triangle-like fashion. Figure 1a shows a current−time transient image of the positive triangle wave signal. The parameters used to establish the positive triangle wave are defined as shown in Figure 1b; $T_P = \frac{(I_{max} - I_{min})}{S_{up}} + \frac{(I_{max} - I_{min})}{S_{down}}$, where T_P is the anodization period, S_{up} and S_{down} are the rates of current rise and fall, respectively. In this experiment, T_P = 30 s, I_{min} = 10 mA, I_{max} = 60 mA, and the slope ratio (S_{up}/S_{down}) is equal to 1.

Figure 2 shows SEM images from the early to latter stage of anodization of a sample prepared using the positive triangle wave current signal, and the period length is about 780 nm. Figure 2a shows the PAA structure at the early stage of the anodization, showing that the PAA film grows irregularly. There are not only channels with incomplete growth but also channels with modulated pore diameter structures. As shown in the inset of Figure 2a, the maximum pore diameter difference is about 40 nm. As shown in Figure 2b, at the middle stage of the anodization, the channels are neatly arranged. PAA has the regular modulated pore diameter

https://doi.org/10.1021/acsomega.0c04452
ACS Omega 2021, 6, 7988−7993

structure, and part of the pores generates more slub-like branches. At the latter stage of the anodization, the number of PAA branches greatly reduces and the pore diameter significantly decreases and grows regularly, as shown in Figure 2c. The inset in Figure 2c shows that the film is highly ordered and symmetrical, without any branches, and arranged in a neat way, and the maximum pore diameter difference is about 60 nm. Figure 2 shows that the pore diameter decreased from the early stage to the latter stage. According to the oxygen bubble mold, the big pores resulted from oxygen evolution at a high voltage and the small pores resulted from oxygen evolution at a low voltage.[23−25] The voltage decreased at the latter stage, which would lead to a decrease in pore diameter. Figure 2 confirms the periodically modulated pore diameter structure of the PAA film, and the modulation effect is optimal at the latter stage of anodization. We conclude that pores formed by the positive triangle wave signal are characterized as symmetrical geometry along the pore axes. Lee et al.[26] also reached a similar conclusion in their study, that is, a current with symmetrical oscillations generates a symmetrical pore structure.

We exhibit the output voltage−time transient image for explaining the structure change during anodization of the sample in Figure 2 in Figure 3. At the early stage of the anodization, the voltage suddenly increases and stabilizes at the maximum value of 179.9 V. Then, the voltage gradually decreases at the maximum value and oscillates unstably following the oscillation of the current. The large voltage causes irregular growth of the PAA film. As the anodization progresses, at the middle stage, the voltage gradually changes steadily. Therefore, there are both the modulated pore diameter structure and slub-like branches. At the latter stage, the value and the period of voltage change steadily and ΔU (the difference between the maximum voltage and the minimum voltage in each cycle) is almost the same. PAA has a well-grown modulated pore diameter structure. The inset in Figure 3 shows the trend of the peak voltage for 30 cycles. Obtained from the inset, the peak voltage decreases rapidly at the early stage, slowly decreases at the middle stage, and almost remains unchanged at the latter stage. This also explains the change in voltage during anodization, resulting in the generation of different structures of the PAA film, which corresponds to the results in Figure 2.

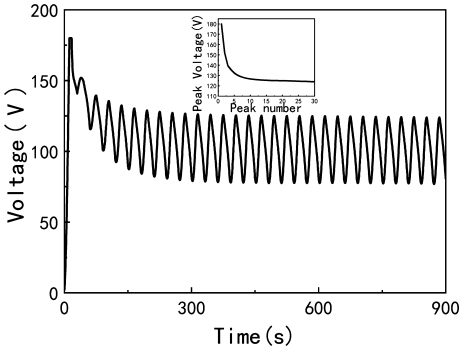

Figure 3. Output voltage (V)−time (t) transient shows the voltage oscillation when I_{min} = 10 mA and I_{max} = 60 mA. The inset shows the trend of peak voltage for 30 cycles.

We prepared samples with the maximum current value of 20, 30, 40, 80, and 100 mA for regulating the pore structure. Then, SEM was employed for the microstructure characterization of the samples at the latter stage of anodization. It is concluded that the current amplitude has an important effect on the pore structure of the PAA film.

As shown in Figure 4, a series of SEM images of samples prepared using positive triangle wave current signals are all images at the latter stage of anodization. PAA with different pore structures was obtained by changing the maximum current value. When the amplitude is 20, 30, 40, 60, 80, and 100 mA, the period length is 0.1, 0.18, 0.4, 0.78, 0.65, and 1.25 μm, respectively. In Figure 4a, it is obvious that the pore structure is straight, because of the smaller ΔI ($\Delta I = I_{max} - I_{min}$), which cannot cause the change in the pore diameter. As shown in Figure 4b−d, PAA gradually possesses the modulated pore diameter structure, rather than the structure of straight. It is concluded that the modulated pore diameter structure will appear when ΔI > 20 mA. As shown in Figure 4d, the maximum pore diameter difference is about 60 nm, and the modulation effect of pore diameter is the most obvious. The PAA film has the periodic slub-like branching structure, as shown in Figure 4e,f. We speculate that the slub-like branching structures might be caused by oxygen bubble evolution.[27,28]

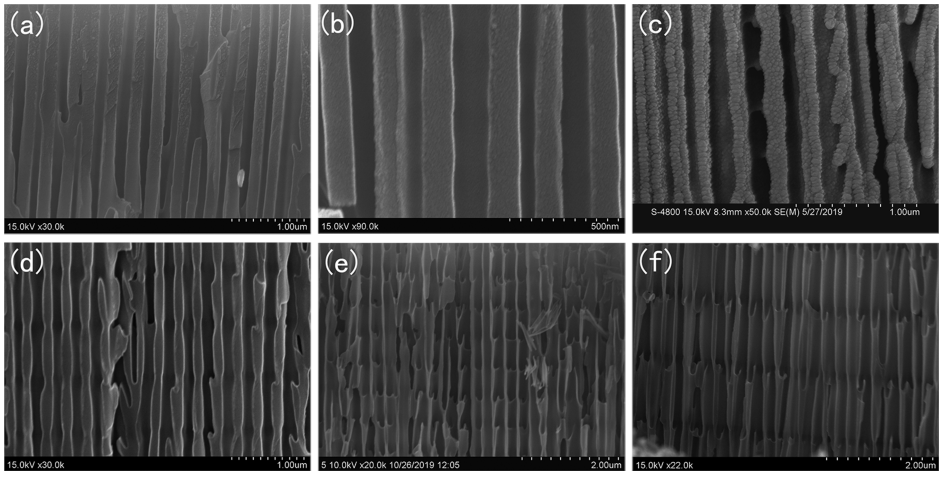

Figure 4. SEM images of the samples prepared using the positive triangle wave current signal. The maximum currents are 20 (a), 30 (b), 40 (c), 60 (d), 80 (e), and 100 mA (f).

https://doi.org/10.1021/acsomega.0c04452
ACS Omega 2021, 6, 7988−7993

The periodic release of oxygen bubbles leads to the periodic slub-like branches.

Figure 5 shows the UV reflection spectra of a series of samples prepared using positive triangle wave current signals. It

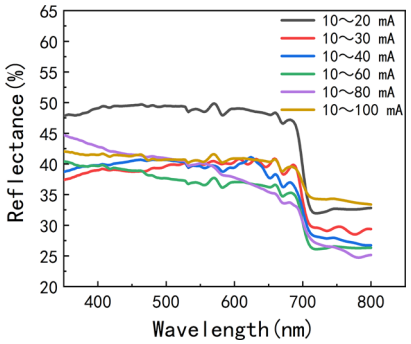

Figure 5. UV reflection spectra of the samples prepared using the positive triangle wave current signal.

can be seen that for visible light with a wavelength lower than 700 nm, all samples are substantially totally reflected, with the characteristic of broad-band reflection. Obviously, the reflectance of the sample with a current of 10−20 mA is much higher than that of others, and the reflectance of the sample with a current of 10−60 mA is almost the lowest. We speculate that the reason is that the porosity of PAA with a modulated pore diameter structure is much greater than that of straight pore structure PAA. The absorption rate of our transparent samples can be neglected, so the overall transmittance is significantly improved for the samples (10−60 mA) with a modulated pore diameter structure. That is, the more obvious the modulation effect is, the higher the transmittance and the lower the reflectance are.

We applied the LabVIEW development environment to make new waveforms, the aforementioned discontinuous sawtooth waves and modified sawtooth waves (the combination of sawtooth waves and sine waves), for exploring the effect of different current waveforms on the structure of the PAA film.

Figure 6a is a SEM image of the sample prepared using a discontinuous sawtooth wave signal, with a period length of 1.32 μm and a branch length of 0.25 μm. Figure 6b is a SEM image of the sample prepared using a modified sawtooth wave signal, with a period length of 1.82 μm and a branch length of 0.33 μm. The insets of the two figures are images of PAA channels grown with a periodic current signal. From the insets, it is found that the PAA film generates V-shaped structures at the junction of adjacent oxide layers (the upper part marked by the blue solid line). The difference is that the lower part structure of the former is the straight shape (the lower part marked by the blue solid line), while the middle and lower part structure of the latter is the straight−branch−straight shape (marked by the blue dotted line). We will explain the growth of the channels with the current and voltage waveforms below.

Figure 7 shows the relationship images of current−time and voltage−time and enlarged images of one cycle. The enlarged images of Figure 7 show that at the first stage, the two current waveforms (black line segments) have the same shape, that is, the sawtooth waveform and the output voltage waveforms (red curve) are also of the same shapes. Therefore, according to our speculation, the signal should generate the same structure at this stage. It is verified from the insets of Figure 6a,b that there is the same structure, that is, the V-shaped structure (the upper part marked by the blue solid line). At the second stage, the current waveform (black line segments) of the discontinuous sawtooth wave is linear, while the modified sawtooth wave is linear−sinusoidal−linear. As shown in the inset of Figure 6a, at the second stage, the PAA with the straight structure (the lower part marked by the blue solid line) generated by the discontinuous sawtooth wave signal, indicated that the constant current signal generates the straight structure. The PAA with the straight−branch−straight structure (marked by the blue dotted line) generated by the modified sawtooth wave signal is shown in the inset of Figure 6b. We speculate that the reason for branching is that the output voltage of the sinusoidal current signal in the second stage increases abruptly and then decreases continuously. At this time, the space charge in the oxide layer is in the state of excess. The growth of the oxide layer is inhibited, resulting in the continuous decrease of anodization rates. The decrease in the current further inhibits the growth of the barrier layer, and when it is thinned to a certain extent, the branches begin to grow. It can be seen that the PAA structures generated by different current waveforms are different and correspond to each other.

4. CONCLUSIONS

In this article, the cyclic anodization method was used to prepare the PAA film with periodic pore structures, and the structure of the PAA film was regulated by different oscillating current signals. The results show that the current amplitudes of positive triangle wave signals have an important effect on the

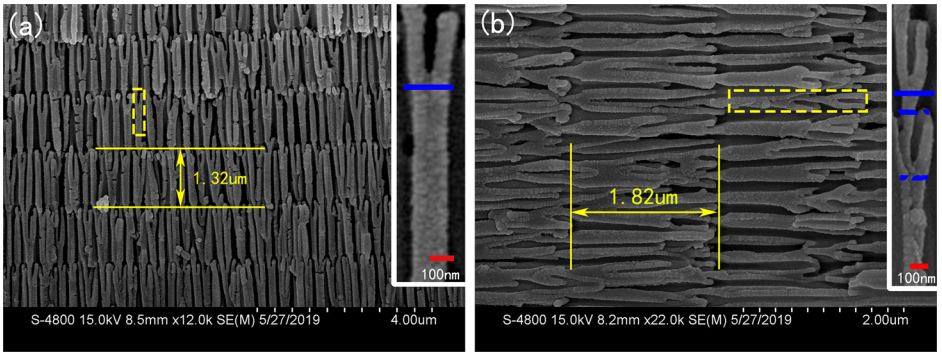

Figure 6. (a) SEM image of the sample prepared using a discontinuous sawtooth wave signal. (b) SEM image of the sample prepared using a modified sawtooth wave signal. [Note: The insets of (a,b) are enlarged images of the yellow dotted frame].

https://doi.org/10.1021/acsomega.0c04452
ACS Omega 2021, 6, 7988−7993

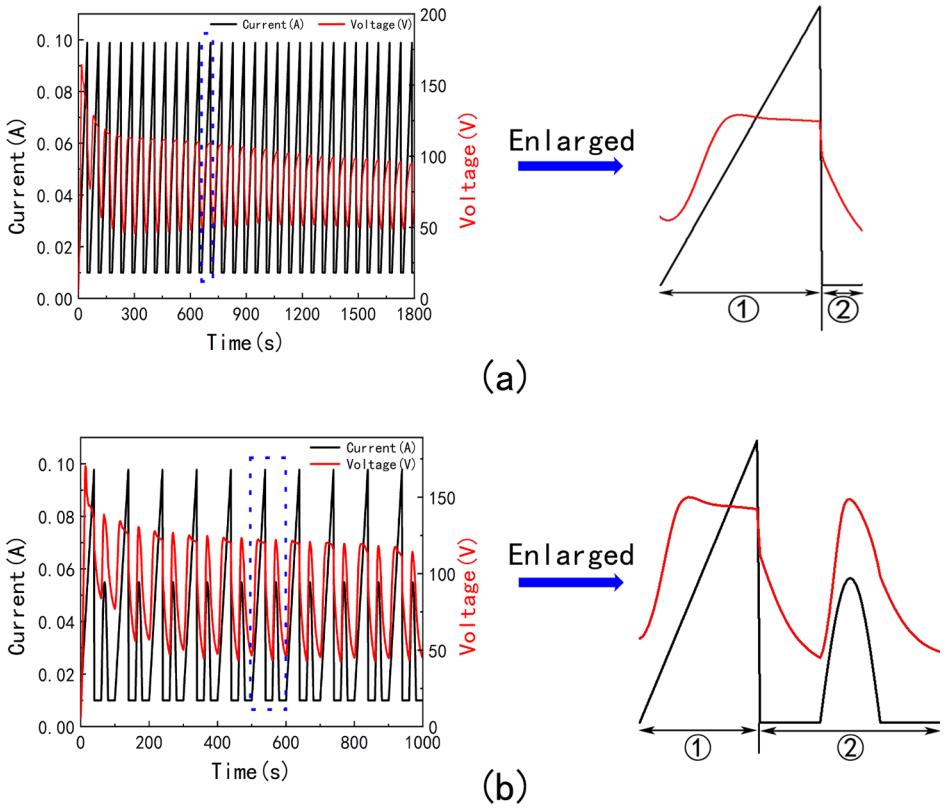

Figure 7. (a) Current (I)−time (t) and voltage (V)−time (t) transients (left) of the discontinuous sawtooth wave signal showing I_{min} = 10 mA and I_{max} = 100 mA, and its enlarged image for one cycle (right). (b) Current (I)−time (t) and voltage (V)−time (t) transients (left) of the modified sawtooth wave signal showing I_{min} = 10 mA and I_{max} = 100 mA, and its enlarged image for one cycle (right).

pore structure of the PAA film. When the maximum current is 30 mA, the PAA film begins to generate a modulated pore diameter structure. When the maximum current is 60 mA, the modulation effect of the pore diameter is the most obvious and the reflectivity is the lowest. The PAA films generated by two different waveform signals with a sawtooth wave have the same V-shaped structure. We found that creating different modes of MA and HA in a single cycle is a pivotal factor in regulating the pore structure. It is feasible to regulate the PAA film structure by changing the parameters such as current waveform profile and amplitude. This method has shown great potential in the preparation of complex PAA structures and the design of novel nanomaterials.

AUTHOR INFORMATION

Corresponding Author

Qin Xu − *Department of Applied Physics, Hebei University of Technology, Tianjin 300401, China;* orcid.org/0000-0003-4541-6539; Email: xuqinzi@126.com

Authors

Tian Lan − *Department of Applied Physics, Hebei University of Technology, Tianjin 300401, China*

Xinjian Xie − *Department of Applied Physics, Hebei University of Technology, Tianjin 300401, China*

Qi Peng − *Department of Applied Physics, Hebei University of Technology, Tianjin 300401, China*

Lu Zhang − *Department of Applied Physics, Hebei University of Technology, Tianjin 300401, China*

Meiyu Dong − *Department of Applied Physics, Hebei University of Technology, Tianjin 300401, China*

Complete contact information is available at: https://pubs.acs.org/10.1021/acsomega.0c04452

Notes

The authors declare no competing financial interest.

ACKNOWLEDGMENTS

This work is supported by the National Natural Science Foundation of China (grant no. 51702083), the Youth Talent Support Program of Hebei Province, the Natural Science Foundation of Hebei Province (Grant nos. A2015202343 and A2019202190), and the China Scholarship Council.

REFERENCES

(1) Xu, D.; Feng, X.; Song, Y.; Li, X.; Zhang, J.; Chen, S.; Shen, X. Fast growth of highly ordered porous alumina films based on closed bipolar electrochemistry. *Electrochem. Commun.* **2020**, *119*, 106822.

(2) Lee, W.; Kim, J.-C. Highly ordered porous alumina with tailor-made pore structures fabricated by pulse anodization. *Nanotechnology* **2010**, *21*, 485304.

(3) Wang, B.; Fei, G. T.; Wang, M.; Kong, M. G.; Zhang, L. D. Preparation of photonic crystals made of air pores in anodic alumina. *Nanotechnology* **2007**, *18*, 365601.

(4) Lee, W.; Scholz, R.; Gösele, U. A Continuous Process for Structurally Well-Defined Al2O3Nanotubes Based on Pulse Anodization of Aluminum. *Nano Lett.* **2008**, *8*, 2155−2160.

(5) Lee, W.; Schwirn, K.; Steinhart, M.; Pippel, E.; Scholz, R.; Gösele, U. Structural engineering of nanoporous anodic aluminium oxide by pulse anodization of aluminium. *Nat. Nanotechnol.* **2008**, *3*, 234−239.

https://doi.org/10.1021/acsomega.0c04452
ACS Omega 2021, 6, 7988−7993

(6) Bruschi, L.; Mistura, G.; Liu, L.; Lee, W.; Gösele, U.; Coasne, B. Capillary condensation and evaporation in alumina nanopores with controlled modulations. *Langmuir* **2010**, *26*, 11894−11898.
(7) Zhao, X.; Meng, G.; Han, F.; Li, X.; Chen, B.; Xu, Q.; Zhu, X.; Chu, Z.; Kong, M.; Huang, Q. Nanocontainers made of various materials with tunable shape and size. *Sci. Rep.* **2013**, *3*, 2416.
(8) Sulka, G. D.; Brzózka, A.; Liu, L. Fabrication of diameter-modulated and ultrathin porous nanowires in anodic aluminum oxide templates. *Electrochim. Acta* **2011**, *56*, 4972−4979.
(9) Lee, W.; Ji, R.; Gösele, U.; Nielsch, K. Fast fabrication of long-range ordered porous alumina membranes by hard anodization. *Nat. Mater.* **2006**, *5*, 741−747.
(10) Wang, X.; Wang, H.; Zhou, Y.; Liu, Y.; Li, B.; Zhou, X.; Shen, H. Confined-space synthesis of single crystal TiO2 nanowires in atmospheric vessel at low temperature: a generalized approach. *Sci. Rep.* **2015**, *5*, 8129.
(11) Zhang, Y.; Liu, M.; Peng, B.; Zhou, Z.; Chen, X.; Yang, S.; Jiang, Z.; Zhang, J.; Ren, W.; Ye, Z. Controlled phase and tunable magnetism in ordered iron oxide nanotube arrays prepared by atomic layer deposition. *Sci. Rep.* **2016**, *6*, 18401.
(12) Kondo, T.; Masuda, H.; Nishio, K. SERS in ordered array of geometrically controlled nanodots obtained using anodic porous alumina. *J. Phys. Chem. C* **2013**, *117*, 2531−2534.
(13) Sauer, G.; Brehm, G.; Schneider, S.; Nielsch, K.; Wehrspohn, R. B.; Choi, J.; Hofmeister, H.; Gösele, U. Highly ordered monocrystalline silver nanowire arrays. *J. Appl. Phys.* **2002**, *91*, 3243−3247.
(14) Meng, G.; Jung, Y. J.; Cao, A.; Vajtai, R.; Ajayan, P. M. From The Cover: Controlled fabrication of hierarchically branched nanopores, nanotubes, and nanowires. *Proc. Natl. Acad. Sci. U.S.A.* **2005**, *102*, 7074−7078.
(15) Wu, Z. H.; Mei, X. Y.; Kim, D.; Blumin, M.; Ruda, H. E. Growth of Au-catalyzed ordered GaAs nanowire arrays by molecular-beam epitaxy. *Appl. Phys. Lett.* **2002**, *81*, 5177−5179.
(16) Lakshmi, B. B.; Patrissi, C. J.; Martin, C. R. Sol−Gel Template Synthesis of Semiconductor Oxide Micro- and Nanostructures. *Chem. Mater.* **1997**, *9*, 2544−2550.
(17) Lee, W.; Yoo, H.-I.; Lee, J. K. Template route toward a novel nanostructured superionic conductor film; AgI Nanorod/γ-Al_2O_3. *Chem. Commun.* **2001**, No. 24, 2530−2531.
(18) Dadras, S.; Aawani, E. Fabrication of YBCO nanowires with anodic aluminum oxide (AAO) template. *Phys. B* **2015**, *475*, 27−31.
(19) Domagalski, J. T.; Xifre-Perez, E.; Santos, A.; Ferre-Borrull, J.; Marsal, L. F. Tailor-engineered structural and physico-chemical properties of anodic alumina nanotubes by pulse anodization: A step forward. *Microporous Mesoporous Mater.* **2020**, *303*, 110264.
(20) Losic, D.; Losic, D., Jr. Preparation of porous anodic alumina with periodically perforated pores. *Langmuir* **2009**, *25*, 5426−5431.
(21) Lee, W.; Schwirn, K.; Steinhart, M.; Pippel, E.; Scholz, R.; Gösele, U. Structural engineering of nanoporous anodic aluminium oxide by pulse anodization of aluminium. *Nat. Nanotechnol.* **2008**, *3*, 234−239.
(22) Losic, D.; Lillo, M.; Losic, D., Jr. Porous alumina with shaped pore geometries and complex pore architectures fabricated by cyclic anodization. *Small* **2009**, *5*, 1392−1397.
(23) Zhu, X.; Song, Y.; Yu, D.; Zhang, C.; Yao, W. A novel nanostructure fabricated by an improved two-step anodizing technology. *Electrochem. Commun.* **2013**, *29*, 71−74.
(24) Zhou, Q.; Tian, M.; Ying, Z.; Dan, Y.; Tang, F.; Zhang, J.; Zhu, J.; Zhu, X. Dense films formed during Ti anodization in NH_4F electrolyte: Evidence against the field-assisted dissolution reactions of fluoride ions. *Electrochem. Commun.* **2020**, *111*, 106663.
(25) Zhou, Q.; Niu, D.; Feng, X.; Wang, A.; Ying, Z.; Zhang, J.; Lu, N.; Zhu, J.; Zhu, X. Debunking the effect of water content on anodizing current: Evidence against the traditional dissolution theory. *Electrochem. Commun.* **2020**, *119*, 106815.
(26) Lee, W.; Kim, J.-C.; Gösele, U. Spontaneous current oscillations during hard anodization of aluminum under potentiostatic conditions. *Adv. Funct. Mater.* **2010**, *20*, 21−27.
(27) Li, D.; Zhao, L.; Jiang, C.; Lu, J. G. Formation of anodic aluminum oxide with serrated nanochannels. *Nano Lett.* **2010**, *10*, 2766−2771.
(28) Yu, M.; Chen, Y.; Li, C.; Yan, S.; Cui, H.; Zhu, X.; Kong, J. Studies of oxide growth location on anodization of Al and Ti provide evidence against the field-assisted dissolution and field-assisted ejection theories. *Electrochem. Commun.* **2018**, *87*, 76−80.

https://doi.org/10.1021/acsomega.0c04452
ACS Omega 2021, 6, 7988−7993